Deep inelastic scattering and forward π^0 production at NLO

P. Aurenche[1], Rahul Basu[2,a], M. Fontannaz[3], R.M. Godbole[4]

[1] Laboratoire d'Annecy-le-Vieux de Physique Théorique LAPTH[b], B.P.110, 74941 Annecy-le-Vieux Cedex, France
[2] The Institute of Mathematical Sciences, Chennai 600 113, India
[3] Laboratoire de Physique Théorique, UMR 8627 CNRS, Université Paris XI, Bâtiment 210, 91405 Orsay Cedex, France
[4] Center for High Energy Physics, Indian Institute of Science, Bangalore 560 012, India

Abstract. We present a detailed phenomenological study of forward hadron (π^0) production in deep inelastic scattering, with both the direct and the resolved contributions calculated to NLO accuracy. A comparison of the theoretical predictions for the various distributions with the H1 data and a study of the stability of the QCD predictions under changes of scales is the focus of this study. We obtain a very good overall description of the recent H1 data with the choice of scale $Q^2 + E_\perp^2$, in contrast to the $(Q^2 + E_\perp^2)/2$ required earlier when the resolved contribution was included only at LO accuracy. We find a more modest variation of the predictions, as the scale is changed from $(Q^2 + E_\perp^2)/2$ to $2(Q^2 + E_\perp^2)$, as compared to the case where the resolved contribution was included only at LO accuracy. This variation is of the order of the rather large experimental errors. Unfortunately, this fact prevents us from concluding that perturbation theory gives an unambiguous prediction for forward particle production in deep inelastic scattering. However, the overall success of perturbative QCD in explaining the small x_{Bj} data means that perhaps a full resummation of the BFKL ladder is not called for. We notice the need for rather large resolved contributions to explain the data at low x_{Bj} even at somewhat larger Q^2 values.

1 Introduction

Recent experimental data, from the H1 collaboration [1], on large transverse energy hadron production in deep inelastic scattering have generated several theoretical papers attempting to explain the data within the framework of perturbative quantum chromodynamics in the next-to-leading order (NLO) approximation. These experimental results confirm and extend older data from H1 [2,3] and ZEUS [4,5]. Since these H1 and ZEUS data on forward hadrons as well as the data on forward jet [6–8] production at large transverse momentum probe the small Bjorken-x_{Bj} region, it was argued [9] that they would be ideally suited to probe the Balitsky–Fadin–Kuraev–Lipatov [10] (BFKL) regime, where the resummation of $\ln(1/x_{Bj})$ terms is important, and that they would show the breakdown of the Dokshitzer–Gribov–Lipatov–Altarelli–Parisi [11] (DGLAP) regime. In this respect the single hadron data are more relevant than the jet data since they cover a lower Bjorken-x_{Bj} range, down to $x_{Bj} = 4 \times 10^{-5}$ [1]. These data are also expected to be more accurate than the jet data because of the difficulty of jet identification at low transverse momentum and in the forward region.

A comparison of older H1 [2] results on single π^0 production, with a model based on lowest order matrix el-

ements and parton cascades [12], shows very strong disagreement between data and theory. The model falls much below the data (a factor 5 to 10 at low Q^2 and low x_{Bj}) and, besides, the shape of the x_{Bj} dependence is incorrect. Adding the contribution where the virtual photon is resolved [13] reduces somewhat the disagreement at large Q^2 but falls short of the data at small Q^2 unless a very large scale is chosen in the evaluation of the anomalous photon component [1]. However, predictions based on improved leading order BFKL dynamics [14] show a better overall agreement when compared to H1 data, specially at low Q^2, but they do not describe the Q^2 evolution correctly [1].

The recent theoretical developments concern mainly the calculation of the single hadron production in the NLO approximation [15–19]. Higher order diagrams neglected in the earlier approaches modify the picture in several ways. They generate new topologies and new hard scattering processes which should be considered as new Born terms. For example, at the lowest order (LO) the hard scattering terms are mediated by quark exchange while in the NLO approximation processes with gluon exchange appear and these become specially important [17] in the forward region where the presence of the gluon pole enhances such terms. Also, at NLO, terms associated with the $q\bar{q}$ collinear component of the virtual photon, which build up the photon structure function (the so-called re-

[a] e-mail: rahul@imsc.res.in
[b] UMR 5108 du CNRS, associée à l'Université de Savoie

solved component), appear. As is well known, a "large" logarithm arises, asymptotically of type $\ln(E_\perp^2/Q^2)$ when $E_\perp^2 \gg Q^2$ ($E_\perp$ is the hadron transverse momentum in the γ^*–proton center of mass frame[1]), and is associated with this structure function, specially when the photon virtuality is small. This term can then be considered a leading order term although it technically appears when calculating higher order diagrams [20]. This is the reason why it was introduced in [13] where it indeed helped improve agreement with the data. However, using a large scale in the photon structure function to enhance the resolved contribution appears artificial. Indeed in an NLO calculation, the increase of the Born resolved contribution is compensated by a decrease of the higher order direct contribution, not included in [13], in such a way that the sum is more stable under changes of scales.

It should be stressed that single hadron production in deep inelastic scattering experiments presents a very stringent consistency test of perturbative QCD and its various input distributions: it involves the proton structure function as well as the hadronic fragmentation functions, all quantities rather precisely measured in other experiments. As just discussed it is also very sensitive to the virtual photon structure function [21–23], which is less well known but which has been recently discussed in detail in [19].

The common features of recent NLO calculations [15–18] are the following. The cross section contains two (complicated) pieces: the "direct" cross section, where the virtual photon couples directly to the hard process, and the "resolved" cross section, where the photon acts as a composite object which is a source of collinear partons taking part in the hard subprocess. The direct contribution is calculated in the NLO approximation, i.e. up to $\mathcal{O}(\alpha_s^2)$, while the cross section involving the resolved component is calculated to lowest order (LO) accuracy with the photon scale compensating term included in the higher order part of the direct piece. No DGLAP type resummation is performed on the virtual photon structure function. Using modern proton structure functions [24,25] and fragmentation functions [26] a very good agreement is achieved with the data when using a common (renormalization, factorization and fragmentation) scale set equal to $(Q^2 + E_\perp^2)/2$. However all the above calculations exhibit the same large scale dependence of the predictions mainly associated with the renormalization scale as will be seen below. A rather large sensitivity of the predictions to the fragmentation functions is also observed, with the data clearly favoring [16], like other hadronic data, the parametrization of Kniehl, Kramer and Pötter [26] (KKP) over that of Kretzer [27]. Furthermore, in [17] a discussion is given to isolate the origin of the large corrections terms and it is found that they are associated with processes with a gluon exchange which are interpreted as the Born terms of the BFKL ladder. The theoretical papers differ in the procedure to obtain the cross section: in [15,16] a calculation of the single particle spectrum is performed with the infrared divergences compensated analytically while in [17,

18] a Monte Carlo generator at the partonic level is constructed with a numerical compensation of divergences.

In [19], the first evaluation, at the NLO accuracy, of the resolved contribution is presented: it includes both the construction and the use of the NLO virtual photon structure function as well as the NLO calculation of the hard matrix elements for the resolved processes. In the limited phenomenological analysis performed, good agreement with the data is obtained with the scale $(Q^2 + E_\perp^2)$, larger than that of the previous NLO calculations. The importance of the resolved contribution to the cross section is again emphasized and it is shown that its factorization scale dependence is reduced at the NLO accuracy compared to the LO calculation. It is then expected that the full cross section will be less scale sensitive than in the work of [15–18].

In the following we present a detailed phenomenological study of hadron production in deep inelastic scattering with both the direct and resolved contributions calculated at NLO accuracy. A special emphasis will be put on the study of the scale variation of the cross section to determine the domain where the perturbative QCD approach is reliable, i.e. stable under changes of scales.

In the next section we set up the theoretical framework and discuss the instabilities related to the various scales introduced in the calculation (factorization scale M on the proton side and M_γ on the photon side, fragmentation scale M_F and factorization scale μ). A detailed comparison with the various experimental H1 distributions [1] is performed next: at small Bjorken-x_{Bj} the large corrections are found to be related to BFKL-like terms which appear in the NLO calculation in some approximation (first corrections in $\alpha_s \ln(1/x_{Bj})$). Studying the Q^2 dependence of the cross section will probe the photon structure function as it is expected to play a dominant role at low Q^2 while at large Q^2 the direct term is expected to dominate. Finally, studying the rapidity η_π or $x_\pi = E_\pi^{lab}/E_p^{lab}$ distributions, as well as the transverse momentum distribution of the pion will help constrain the quark and gluon fragmentation into pions.

Hadron production in DIS experiments offers a very rich structure: it is a problem with two scales, Q^2 and $E_\perp^2$, with a large variation in the ratio of these two scales allowing for the testing of the theoretical results in different regimes. Furthermore, the small Q^2 limit makes it possible to make contact with photoproduction experiments. Combining all the data will help in understanding the nonperturbative input to the photon structure function and its decreasing importance when the virtuality of the photon increases. It will give some insight on the transition from the non-perturbative to the perturbative regime, for the photon structure function.

2 Theoretical framework

We first discuss the features of the resolved cross section which were not taken into account in the previous papers [15–18]. When calculating the higher order (HO)

---

[1] The variable which we denote $E_\perp$ here is called p_T^* in [1].

corrections to the direct contribution there appear configurations where the virtual photon turns into an almost collinear q–$\bar{q}$ pair with the quark or the antiquark subsequently interacting with a parton from the proton. This HO contribution, in principle negligible for $E_\perp^2$ close to Q^2, is important when $E_\perp^2$ becomes large. In this case we cannot content ourselves with the lowest order expression of the quark distribution in the virtual photon, proportional to $\ln(E_\perp^2/Q^2)$. The latter must be replaced by a resummed LO or NLO expression. The standard procedure consists in subtracting from the HO corrections a term proportional to $\ln(M_\gamma^2/Q^2)$ and to calculate a resolved contribution with fully evolved parton distributions at the factorization scale M_γ^2. The M_γ^2 dependence of the resolved part is partly compensated by the $\ln(E_\perp^2/M_\gamma^2)$ counterterm which remains in the direct HO contribution. In [19] it was argued that a physical choice for the factorization scale is $M_\gamma^2 = (Q^2 + C_\gamma^2\, E_\perp^2)$ with C_γ of order $\mathcal{O}(1)$. With this scale, the resolved component is negligible when $E_\perp^2 \ll Q^2$, whereas it is large when $E_\perp^2 \gg Q^2$. In the latter case, we recover the standard factorization scale $C_\gamma^2\, E_\perp^2$ of large-$E_\perp$ reactions.

Direct and resolved cross sections, calculated in the NLO approximation, have been discussed respectively in [17,19]. Here, we do not give the technical details of these calculations which can be found in the relevant references, but we summarize the main results that were obtained.

(1) The HO corrections to the direct cross section are very large (in the H1 kinematical domain) and essentially come from graphs containing the exchange of a gluon in the t-channel. These graphs represent a zeroth order approximation to the BFKL ladder.

(2) The NLO direct cross section strongly depends on the renormalization scale μ.

(3) With the factorization scale $M_\gamma^2 = Q^2 + E_\perp^2$ the NLO resolved contribution is as large as the NLO direct one. Therefore we have access, through this contribution, to the parton distributions in the virtual photon.

(4) With the "natural" scale $Q^2 + E_\perp^2$, the total cross section is in good agreement with the H1 data, thus suggesting that a sizeable BFKL type contribution may not be necessary to explain the data.

The second point above is important because it does not allow us to make stable predictions for the cross section and to assess the need for other contributions of the BFKL type. Preliminary studies of the renormalization scale dependence have been performed separately, for the direct cross section [17] and the resolved cross section [19]. Here we would like to do a more complete study of the scale sensitivity of the total cross section, including also the effects of the various factorization scales. As is well known, only the total cross section has a physical meaning. The separate contributions, Born terms, HO terms, direct or resolved terms are all factorization and renormalization scale dependent. Since the direct and resolved NLO cross section are available, such a study of the scale sensitivity is now feasible.

Before starting this study let us specify the various building blocks of the total cross section. For the par-
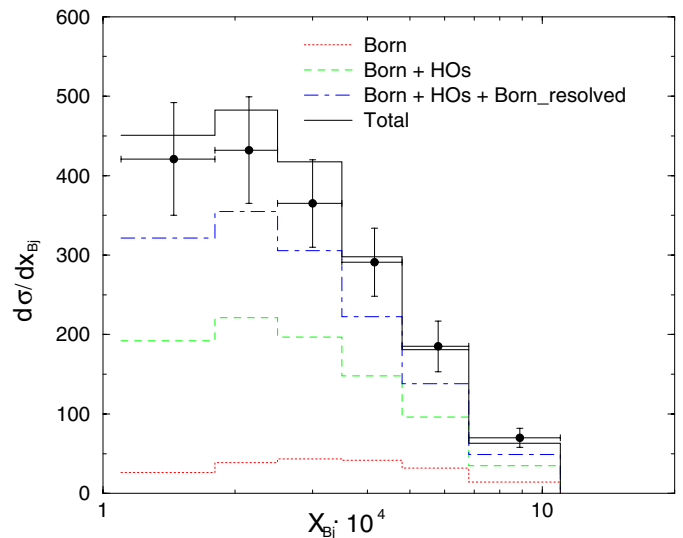

Fig. 1. The cross section $d\sigma/dx_{\mathrm{Bj}}$ corresponding to the range $4.5\,\mathrm{GeV}^2 \leq Q^2 \leq 15\,\mathrm{GeV}^2$ and $E_\perp > 2.5\,\mathrm{GeV}$ compared to H1 data [1]. Cuts on all the other kinematical variables are given in the text. The symbol HO_s denotes the direct HO correction from which the lowest order resolved contribution has been subtracted

ton distributions in the proton, we use the CTEQ6M tables [25], and for the distributions in the virtual photon the parametrization given in [19]. In the latter this parametrization was used with fixed value of Q^2 corresponding to the average value $\langle Q^2 \rangle$ observed in a cross section. For instance for the cross section $d\sigma/dx_{\mathrm{Bj}}$ in the range $4.5\,\mathrm{GeV}^2 \leq Q^2 \leq 15\,\mathrm{GeV}^2$ (see Fig. 1), we used $\langle Q^2 \rangle = 8\,\mathrm{GeV}^2$. This value corresponds to the overall bin $1.1 \times 10^{-4} \leq x_{\mathrm{Bj}} \leq 11.0 \times 10^{-4}$. However this value changes with x_{Bj} and the description of the whole x_{Bj} domain by a single value $\langle Q^2 \rangle$ is not accurate. Therefore in this paper we use a parametrization depending continuously on x_{Bj}, Q^2 and M_γ^2. We work in the $\overline{\mathrm{MS}}$ renormalization and factorization schemes and all the scales are equal to $(Q^2 + E_\perp^2)$. We take $n_f = 4$ flavors and for $\alpha_s(\mu)$ we use an exact solution of the two-loop renormalization group equation with $\Lambda_{\overline{\mathrm{MS}}} = 326\,\mathrm{MeV}$. The fragmentation functions of the partons in π^0 are those of [26]. With this input we obtain the cross section displayed in Fig. 1 and compared with H1 data measured in the range $4.5\,\mathrm{GeV}^2 \leq Q^2 \leq 15\,\mathrm{GeV}^2$ [1]. Our calculations are performed at $\sqrt{S} = 300.3\,\mathrm{GeV}$ and the forward-π^0 cross section is defined with the following cuts. In the laboratory system a π^0 is observed in the forward direction with $5° \leq \theta_\pi \leq 25°$; the laboratory momentum of the pion is constrained by $x_\pi = E_\pi^{\mathrm{lab}}/E_p^{\mathrm{lab}} \geq 0.1$, and an extra cut is put on the π^0 transverse momentum in the γ^*–p center of mass system: $E_\perp > 2.5\,\mathrm{GeV}$. The inelasticity $y = Q^2/x_{\mathrm{Bj}}S$ is restricted to the range $0.1 < y < 0.6$. We clearly observe in this figure the points (1), (3) and (4) mentioned above, and in particular, the very large HO_s (the index s means that the lowest order resolved component has been subtracted from the HO corrections to the
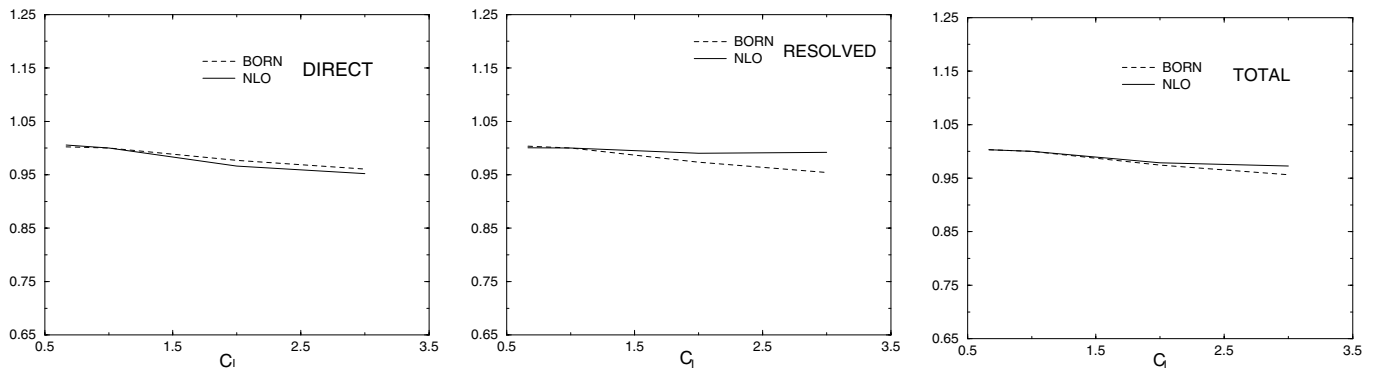
Fig. 2. Cross section variations with C_I which has been defined in the text. The cross sections are normalized to 1.0 at $C_\mathrm{I} = 1$. The choice of kinematic conditions is the same as in Fig. 1
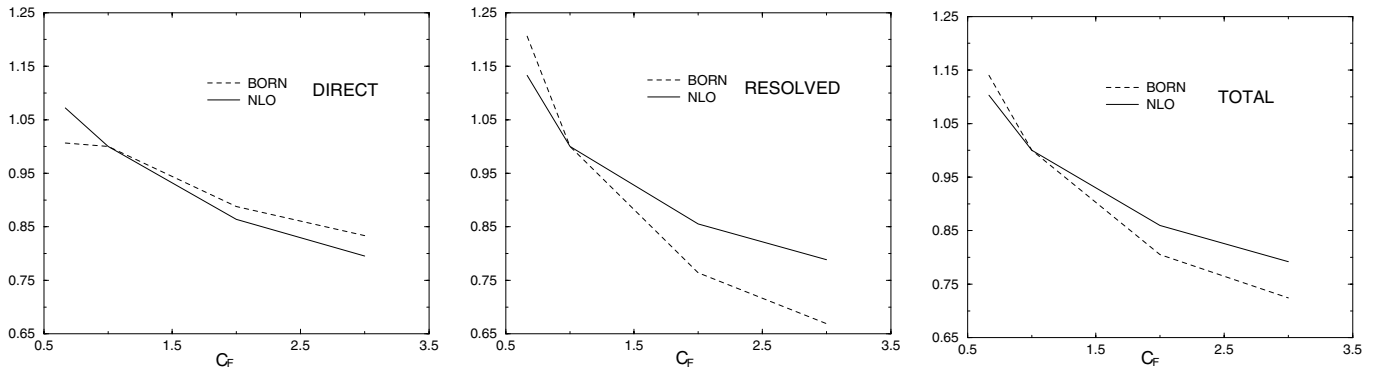

Fig. 3. Cross section variations with C_F which has been defined in the text. The cross sections are normalized to 1.0 at $C_\mathrm{F} = 1$. The choice of kinematic conditions is the same as in Fig. 1

direct term, as discussed at the beginning of this section). We also notice the importance of the HO corrections to the resolved cross section. With respect to the corresponding figure of [19], we note that the resolved component is larger at small x_Bj and smaller at large x_Bj, which improves agreement with data at large x_Bj. This is due to the fact that the average $\langle Q^2 \rangle$ is smaller at small x_Bj than at large x_Bj. Figure 1 is the starting point of our scale studies. We choose a kinematic region for which the HO corrections are large (this is due to the small value of $E_\perp > 2.5\,\mathrm{GeV}$) in order to better exhibit the scale dependence, but with the consequence (as we shall see) that the cross section does not stabilize for an optimum choice of the scales. Let us define the factorization scales $M_k^2 = C_k^2(Q^2 + E_\perp^2)$ where k stands for I (the proton distribution scale) or F (the fragmentation function (FF) scale). We also introduce the virtual photon factorization scale $M_\gamma^2 = Q^2 + C_\gamma^2 E_\perp^2$ and the renormalization scale $\mu^2 = C_\mu^2(Q^2 + E_\perp^2)$.

We study the sensitivity of the various components of Fig. 1 in the single bin $1.1 \times 10^{-4} < x_\mathrm{Bj} < 11.0 \times 10^{-4}$ and start with the factorization scales M_I and M_F. In Figs. 2 and 3, we observe a very different behavior. The variation with M_I is almost flat whereas that with M_F is strongly decreasing. These differences are due to the different average values of x_p, the proton distribution variable, and z, the fragmentation function variable, corre-

sponding to the kinematics of Fig. 1. In the direct process for instance, we have $\langle x_p \rangle \sim 0.1$, a domain in which the proton distribution functions do not vary much with M_I. For the fragmentation variable we have $\langle z \rangle \sim 0.3$ in the direct case, and $\langle z \rangle \sim 0.7$ in the resolved case. In these ranges, the variation of the fragmentation functions $D(z, M_\mathrm{F})$ are not negligible; the higher the value of z, the stronger the variation. Hence the different behavior of the direct and resolved contributions. Moreover in the direct case, we observe that the HO corrections do not compensate the Born term variation. This is due to the fact that the HO corrections contain new channels which appear as new Born contributions for which there are no compensating $\ln(M_\mathrm{F}/E_\perp)$ terms. For instance, we have the opening of the new channel corresponding to Fig. 4a with the final gluon fragmenting into a π^0. At NLO there is no counterterm which corrects this new Born contribution. Such terms would only appear at NNLO. The contribution of this new channel, involving the exchange of a gluon in the t-channel, is very large and the overall behavior of the NLO cross section is very similar to that of the Born contribution. In the resolved contribution a graph with a gluon exchanged in the t-channel already exists at the Born level and the HO corrections contain the appropriate counterterm. However the compensation between the
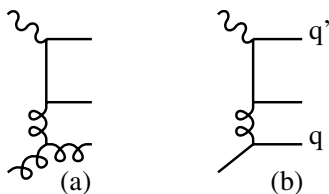
Fig. 4. Examples of HO graphs leading to the opening of new channels when the final hadron is a fragment of the gluon or of the quark q

Born contribution and the HO is not complete due to the large values of $\langle z \rangle$ involved.

Let us now turn to the study of the variations with M_γ which are displayed in Fig. 5. In the variations studied till now, there was no compensation between the resolved and the direct terms. For instance, the M_I dependence of the parton distributions in the photon were separately compensated by $\ln(M_I/E_\perp)$ terms which appear in the direct or in the resolved HO corrections. However, for M_γ, we have compensation between the resolved and the direct terms that we can observe in Fig. 5. When M_γ increases the Born + HO$_\text{s}$ direct contribution decreases. This is due to the fact that a term proportional to $\log(M_\gamma/Q)$ is subtracted from the HO corrections leaving a piece $\log(E_\perp/M_\gamma)$ in the remaining HO$_\text{s}$ part, as explained at the beginning of this section. On the other hand, the resolved contribution increases with the increase of the parton distributions in the virtual photon. A counterterm present in the HO resolved correction dampens the variation of the NLO cross section compared to the Born case. More precisely, the scale variation of the photon structure function contains two pieces (see e.g. (16) in [19]): the inhomogeneous part, proportional to α, and the homogeneous or hadron-like part proportional to $\alpha\alpha_\text{s}$. The scale variation of the inhomogeneous part is compensated by the HO$_\text{s}$ direct term, while that of the homogeneous part is in the HO resolved contribution. For a consistent calculation it is therefore necessary to work at the NLO level for both direct and resolved pieces. Due to the compensation between the direct and the resolved contributions,

the total cross section exhibits a smoother behavior when M_γ^2 varies by a factor 20.

Finally let us consider the variations as a function of the renormalization scale μ. They are the largest. We note the same phenomenon as observed for the M_F-scale variation: no compensation for the direct NLO term and a small compensation for the NLO resolved contribution. Concerning the direct term, this behavior again arises due to the opening of new channels, without virtual corrections (they appear only at NNLO), containing terms in $\log(\mu/E_\perp)$ to compensate the μ dependence of $\alpha_\text{s}(\mu)$. As these new Born terms are proportional to $\alpha_\text{s}^2(\mu)$ and constitute a large part of the cross section [17], the variation of the latter is strong. On the other hand virtual corrections to terms containing a gluon exchanged in the t-channel are present in the resolved contribution. This produces the small effect observed in Fig. 5 and we do not find any reasonable value of μ for which the cross section would reach an optimum. This is due to the large HO corrections corresponding to the small values of the transverse energy in the H1 kinematical domain studied here. Indeed the H1 experiment puts a minimum cut-off on $E_\perp$ (the transverse energy in the γ^*–proton center of mass frame) of 2.5 GeV. This is a small value for a "large-p_T" reaction and the resulting HO are large. However for higher values of the cut-off, the HO corrections are smaller and we find a μ variation of the resolved cross section which exhibits an optimum (maximum) point. For instance in [19] a cut-off $E_\perp > 5$ GeV was used and an optimum of the cross section was found for $C_\mu \sim 0.2$.

Therefore we reach the conclusion that the addition of the NLO resolved component improves the behavior of the cross section with respect to the scale variation. However the sensitivity of the cross section to the renormalization scale variation prevents us from predicting absolute values for the latter. For instance, in the range $1/4 < C_\mu^2 < 4$, the predictions vary by a factor 2. This fact clearly points towards the necessity of calculating NNLO corrections. For the time being with the aim of phenomenological applications in mind, we choose scales which lead to a good description of the data in the range $4.5 \text{ GeV}^2 \leq Q^2 \leq 15 \text{ GeV}^2$. As we can see from Fig. 1, such an agreement is found with all scales set equal to
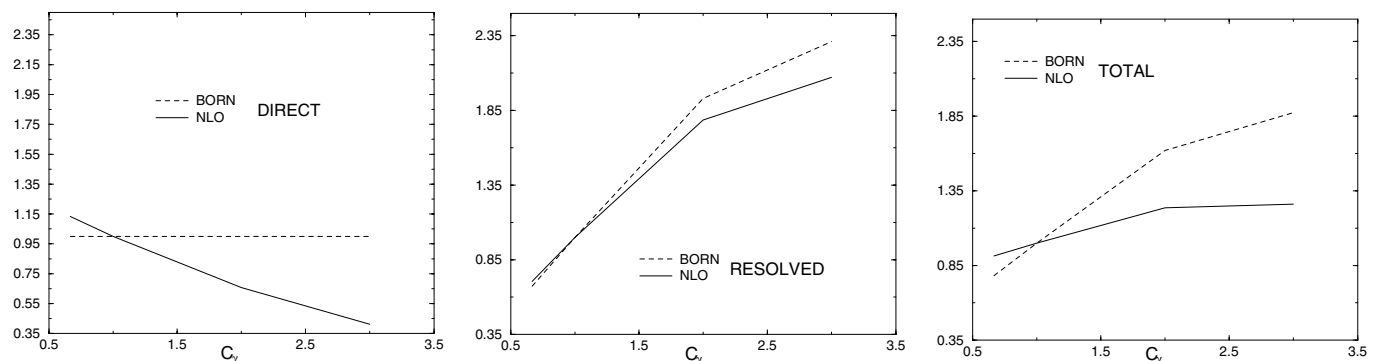

Fig. 5. Cross section variations with C_γ which has been defined in the text. The cross sections are normalized to 1.0 at $C_\gamma = 1$. The choice of kinematic conditions is the same as in Fig. 1
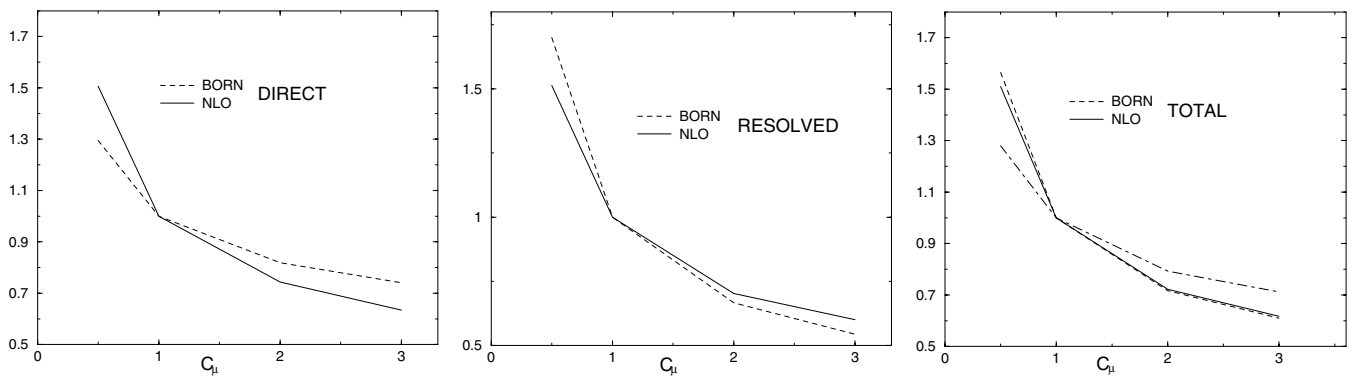
Fig. 6. Cross section variations with C_μ which has been defined in the text. The cross sections are normalized to one at $C_\mu = 1$. The choice of kinematic conditions is the same as in Fig. 1 except for the rightmost panel, where the dash-dotted curve corresponds to the NLO cross section calculated in the bin $20\,\mathrm{GeV}^2 < Q^2 < 70\,\mathrm{GeV}^2$, $3.9 \times 10^{-4} < x_{\mathrm{Bj}} < 6.3 \times 10^{-3}$, $E_\perp > 3.5$ GeV

$Q^2 + E_\perp^2$. Then with the same scales we make predictions for $\mathrm{d}\sigma/\mathrm{d}x_{\mathrm{Bj}}$ in the other Q^2 ranges, as well as for $\mathrm{d}\sigma/\mathrm{d}E_\perp$ and $\mathrm{d}\sigma/\mathrm{d}x_\pi$. Because of the marked scale sensitivity of the cross sections, scales giving a good description of data in a given Q^2 range do not necessarily lead to a good agreement in another range. It turns out, as we shall see, that a satisfactory description of all the data can be obtained with this single choice of scales. Of course the scale choice could be refined in order to improve the agreement between data and theory in Fig. 1, especially at small x_{Bj}. But this is a formal exercise that does not present any physical interest.

Finally, to ameliorate some of our negative conclusions on the scale dependence of the cross section, we note that at larger Q^2 and $E_\perp^2$, the sensitivity to the renormalization scale is reduced. In Fig. 6 (rightmost panel), we display the behavior of the total NLO cross section in the range $20\,\mathrm{GeV}^2 \leq Q^2 \leq 70\,\mathrm{GeV}^2$ with $3.9 \times 10^{-4} < x_{\mathrm{Bj}} < 6.3 \times 10^{-3}$ ($E_\perp > 3.5\,\mathrm{GeV}$). The cross section varies by less than $\pm 25\%$ when C_μ is in the range $1/4 < C_\mu^2 < 4$.

3 Comparison to H1 data

We are now ready to compare the theoretical predictions to the H1 recent results [1] on single π^0 inclusive cross section. The same kinematical cuts as in the experimental data are imposed on the theory, and they are given in the previous section while discussing Fig. 1.

Concerning the theoretical predictions "NLO" will refer to the full next-to-leading logarithmic predictions for the direct term as well as for the resolved term, where "direct" refers to the lowest order ("Born") term with the attached higher order corrections labeled "HO_s" above[2].

---

[2] In [18] an extensive discussion is given of the interference terms where the photon couples to two different quark lines, which leads to triangle graphs when calculating the cross section (the so-called Furry terms) and these terms are found to give an appreciable contribution. In the present calculation, valid for neutral pion production, these terms are not present
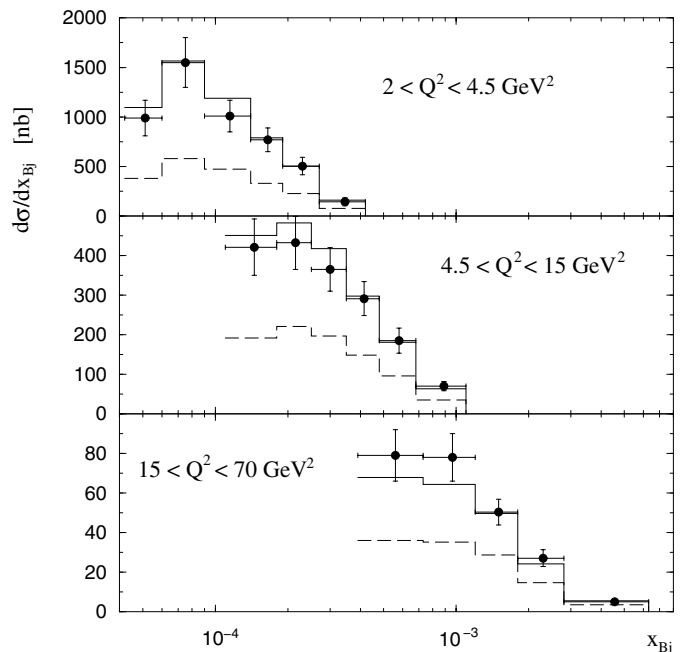

Fig. 7. Inclusive π^0 cross section as a function of x_{Bj} in the range $E_\perp > 2.5$ GeV for three different intervals in Q^2. The cuts on other variables are given in the text. The data points are from the H1 collaboration [1]. The histograms are the theoretical predictions obtained with all scales set equal to $(Q^2 + E_\perp^2)$; solid line: full NLO predictions; dashed line: "direct" contribution

The $\overline{\mathrm{MS}}$ scheme is used throughout with $\Lambda_{\overline{\mathrm{MS}}} = 326\,\mathrm{MeV}$. For convenience we recall here the basic ingredients entering the calculation. All predictions are made using CTEQ6M [25] for the proton parton distributions and KKP [26] for the fragmentation functions of the pion. For the virtual photon structure function, in the resolved term,

---

because the quark production cross section is cancelled by the antiquark cross section. The same reason makes them vanish in jet production.
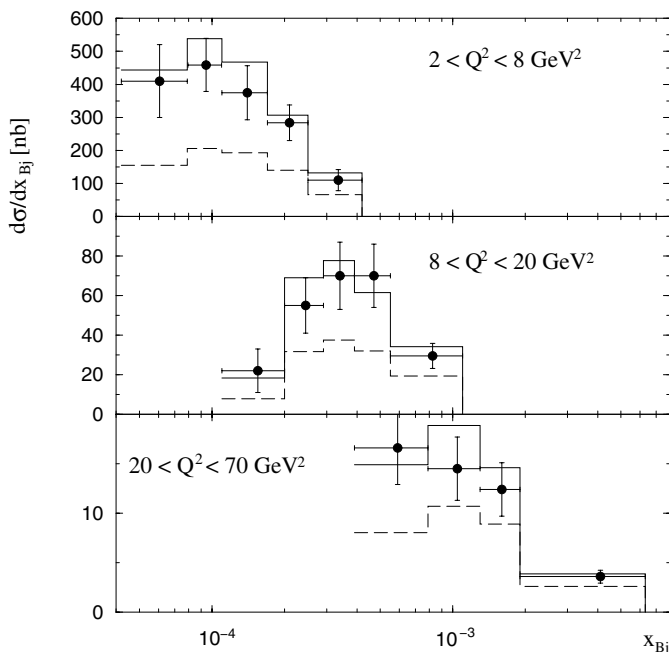
Fig. 8. Inclusive π^0 cross section as a function of x_{Bj} in the range $E_\perp > 3.5\,\mathrm{GeV}$ for three different intervals in Q^2. The cuts on other variables are given in the text. The data points are from the H1 collaboration [1]. The histograms are the theoretical results: the solid line corresponds to full NLO predictions and the dashed line to the "direct" contribution. Choice of scales is as in Fig. 7

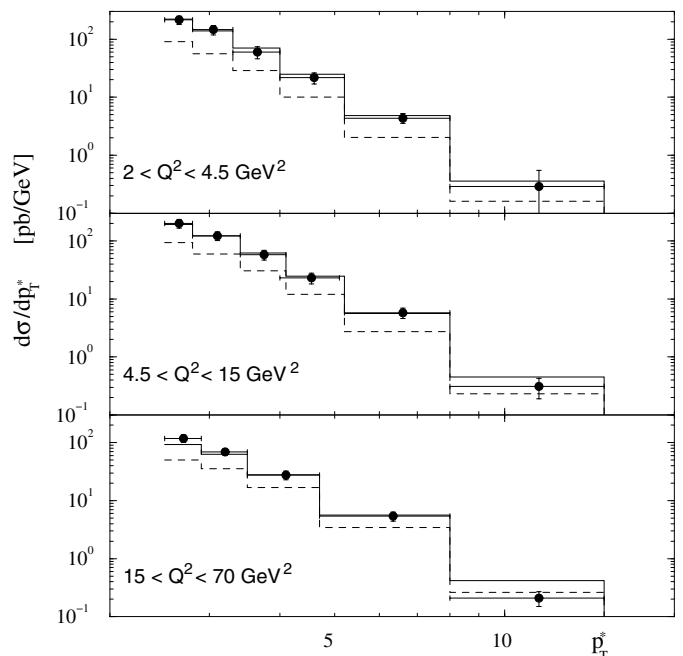**Fig. 9.** Inclusive π^0 cross section as a function of the π^0 transverse momentum in the γ^*–proton center of mass frame for three different intervals in Q^2. The data points are from the H1 collaboration [1]. The histograms are the theoretical results: the solid line corresponds to full NLO predictions and the dashed line to the "direct" contribution. Choice of scales is as in Fig. 7. The variable p_{T}^* in the figure is the notation of the H1 collaboration and is called $E_\perp$ in the text

the recent parametrization of [19] is taken. Using the lowest order approximation (the so-called "box" approximation) changes the results by less than 10%. The common scale is chosen to be $(Q^2 + E_\perp^2)$.

The comparison between theory and experiment for the single pion distribution as a function of x_{Bj} is shown in Figs. 7 and 8 for the cuts $E_\perp > 2.5\,\mathrm{GeV}$ and $E_\perp > 3.5\,\mathrm{GeV}$ respectively. We notice the very good overall agreement between data and theory (note the linear scale) for the whole x_{Bj} range. At a finer level one may observe some systematics in Fig. 7 where at low x_{Bj}, for the medium Q^2 range, the theoretical predictions fall slightly above the data while in the large Q^2 bin it is the opposite. Furthermore, one notes the importance of the resolved contribution (the difference between the solid and the dashed line). At low Q^2 (upper panels) it is 1.5 to 1.9 times the direct contribution, decreasing as x_{Bj} increases, while at large Q^2 (lower panels) it never exceeds the direct term and becomes almost negligible at large x_{Bj}: this is as expected from the discussion in the previous section. The importance of the resolved contribution to obtain agreement with the data was also pointed out by Kramer and Pötter who calculated the NLO cross section (resolved term at leading order) to forward dijet production [28] and compared it with H1 [3] and ZEUS [7] data, as well by Jung and collaborators [29] in their analysis using a LO calculation. One may comment again on the rather unusual situation at low x_{Bj} where the HO$_\mathrm{s}$ correction to the direct term can be up to an order of magnitude larger than

the Born term (see Fig. 1) due to the appearance of the BFKL-like terms of Fig. 4 with gluon poles. At large x_{Bj} however one recovers the "usual" situation where the HO$_\mathrm{s}$ piece is of the same order of magnitude as the lowest order term.

A very impressive agreement is also achieved, in Fig. 9, for the $E_\perp$ spectrum for all Q^2 values. The resolved contribution decreases with Q^2 but it remains important for all values of Q^2 and all transverse momenta. The $E_\perp$ distribution should be sensitive to the choice of the fragmentation functions and it is interesting to try different sets, in particular that of Kretzer [27]. We do not do it here as it has already been shown by Daleo et al. [16] that the parametrization of [27] leads to predictions which fall below the data. This confirms previous studies [30] showing that the fragmentation functions of [27] systematically underestimate particle production in hadronic reactions.

Similarly, the longitudinal momentum distribution of the pion is in remarkable agreement with the data both for specific Q^2 bins (Fig. 10) or specific x_{Bj} bins (Fig. 11). Again the resolved component is important over the whole x_π range but, clearly, it gives a decreasing contribution as Q^2 increases. One has to note that there is little correlation between x_π and the fragmentation variable z: for instance, in the resolved case $\langle z \rangle \sim .5$ (calculated with the Born term only in the region $2\,\mathrm{GeV}^2 < Q^2 < 4.5\,\mathrm{GeV}^2$) varies by less than 10% when x_π varies between the first and the last bin of Fig. 10. Therefore we cannot rely on the
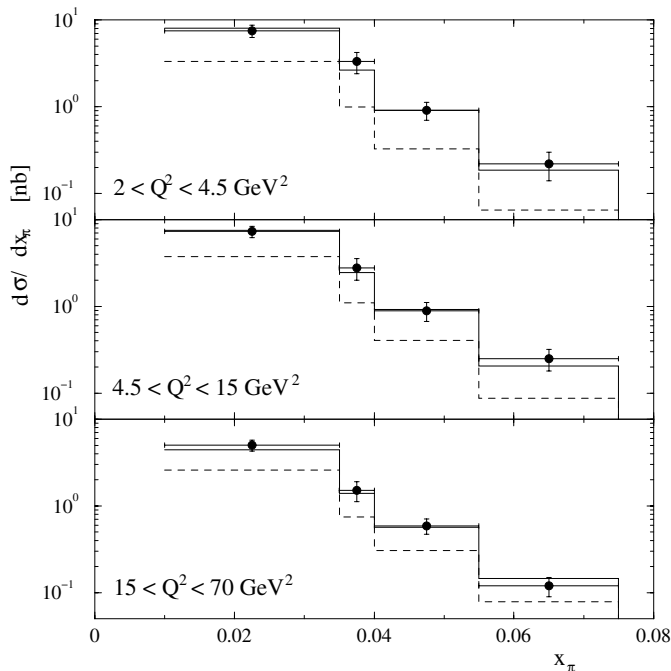
Fig. 10. Inclusive π^0 cross section as a function of $x_\pi = E_\pi^{\text{lab}}/E_p^{\text{lab}}$ in the range $E_\perp > 2.5$ GeV for three different intervals in Q^2. The cuts on the other variables are given in the text. The data points are from the H1 collaboration [1]. The histograms are the theoretical results:the solid line corresponds to full NLO predictions and the dashed line to the "direct" contribution. Choice of scales is as in Fig. 7

Fig. 11. Inclusive π^0 cross section as a function of $x_\pi = E_\pi^{\text{lab}}/E_p^{\text{lab}}$ in the range $E_\perp > 2.5$ GeV for three different intervals in x_{Bj}. The cuts on the other variables are given in the text. The data points are from the H1 collaboration [1]. The histograms are the theoretical results: the solid line corresponds to full NLO predictions and the dashed line to the "direct" contribution. Choice of scales is as in Fig. 7

x_π spectrum to constrain the z shape of the fragmentation functions.

From the comparison with data we can conclude that perturbative QCD, in the NLO approximation, gives unexpectedly good results, especially in view of the initial discrepancy observed at leading order between theory and data. Two ingredients explain this fact: the unusually large correction to the direct term, specially at low x_{Bj}, and the importance of the resolved photon contribution including the associated higher order corrections. Unfortunately, none of the inclusive observables discussed here allows for an unambiguous separation of the two terms. In principle, looking at more exclusive quantities, such as hadron–jet correlations, would allow for the determination of the longitudinal momentum fraction in the photon x_γ [31], and consequently the separation of the two types of terms. However, since the HO_s term is very large, it may lead to a large contribution at $x_\gamma \neq 1$ making the separation from the resolved term difficult.

The success of perturbative QCD to explain the data at small x_{Bj} is interesting. It seems to imply that there is no clear signal in the H1 data of the BFKL type resummation effects and that keeping only the lowest order term in the usual perturbative sense is justified. One reason may be the following. The BFKL result is derived for asymptotic energies. However, at HERA the range of the rapidity $\ln(S/Q^2)$ available is not extremely large and
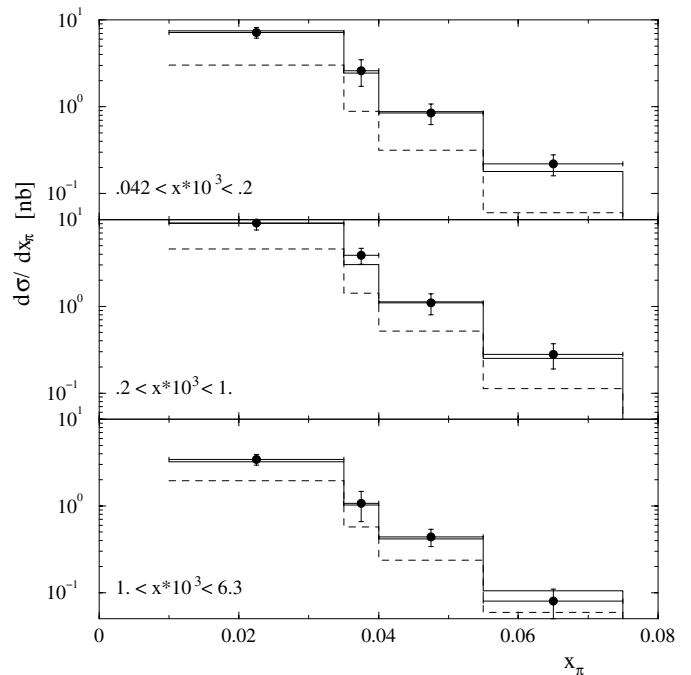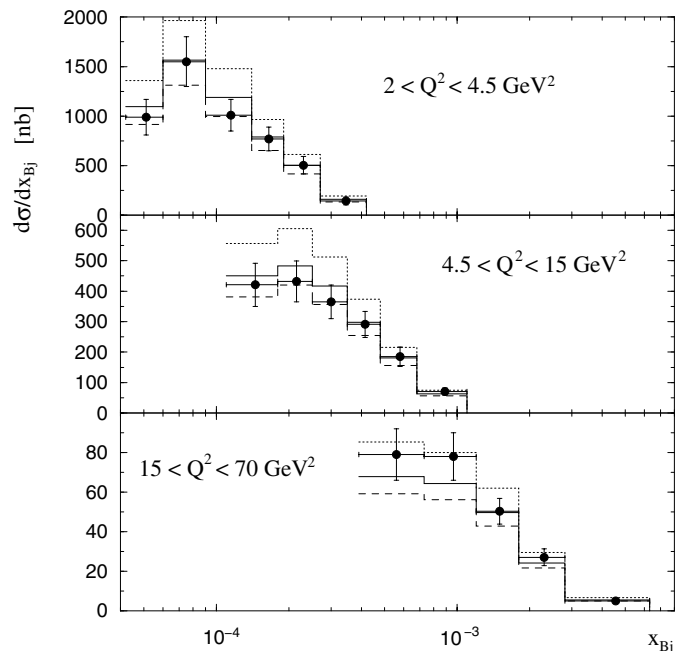

Fig. 12. Inclusive π^0 cross section as a function of x_{Bj} in the range $E_\perp > 2.5$ GeV for three different intervals in Q^2. The data points are from the H1 collaboration [1]. The histograms are the NLO theoretical results for different scales of the form $C^2(Q^2 + E_\perp^2)$: $C^2 = .5$, upper dotted histogram; $C^2 = 1$, solid histogram; $C^2 = 2$ lower dashed histogram
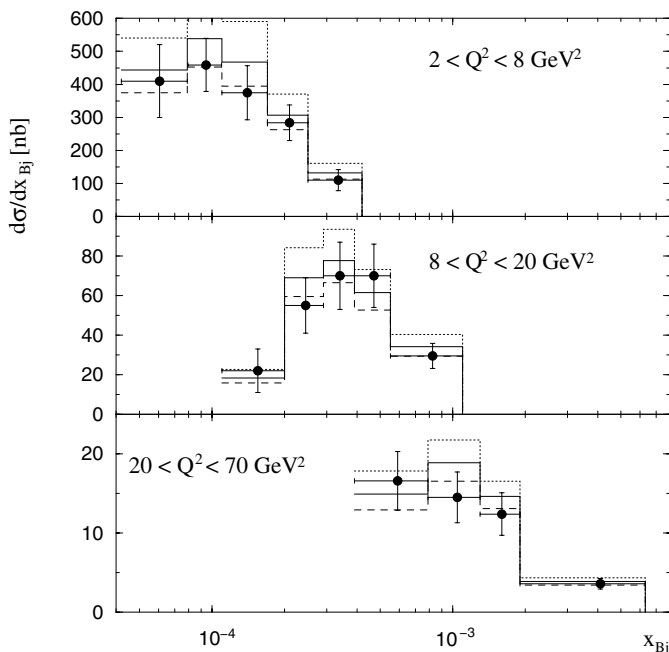
Fig. 13. Inclusive π^0 cross section as a function of x_{Bj} in the range $E_\perp > 3.5\,\mathrm{GeV}$ for three different intervals in Q^2. The data points are from the H1 collaboration [1]. The histograms are the NLO theoretical results for different scales of the form $C^2(Q^2 + E_\perp^2)$: $C^2 = .5$, upper dotted histogram; $C^2 = 1$, solid histogram; $C^2 = 2$ lower dashed histogram

threshold effects do not allow for the full formation of the BFKL ladder [32,33].

4 Comparison with other perturbative calculations

The H1 data are also in very good agreement with the NLO calculations of Daleo et al. [16] and Kniehl et al. [18]. We recall that the difference between these approaches and the present one lies in the fact that, in the former, no special consideration is given to the photon structure function: the NLO correction to the direct term contains a "large" factor of type $\ln((Q^2 + E_\perp^2)/Q^2)$ which amounts, in fact, to parametrizing the photon function by its lowest perturbative approximation. Furthermore no NLO corrections are included in the resolved cross section. In contrast, in this work, we use both a NLO expression for the resolved photon structure function and we include the HO corrections to the resolved cross section. Agreement with the data is obtained in all cases at the cost of using a different choice for the common scale. In [16,18], as well as in our previous work [17], the scale $(Q^2 + E_\perp^2)/2$ was the appropriate choice. In this work, it is seen that the scale $(Q^2 + E_\perp^2)$ is preferred. The data do not obviously prefer one or the other of the two sets of calculations as the shape of the observables is not affected. In [18] a very large scale sensitivity was however observed: under the rather modest change from $(Q^2 + E_\perp^2)/4$ to $(Q^2 + E_\perp^2)$ the theoretical predictions vary by as much as a factor 2 in

some cases, and, in any case, the theoretical uncertainties are much (sometimes twice) larger that the experimental ones (statistic and systematic errors combined). In the current approach we expect a smaller sensitivity to the scales since more HO corrections are taken into account. Besides, it is seen from Figs. 3, 5 and 6 that the variation with the scales seems to decrease at higher scales. This is illustrated in Figs. 12 and 13 where we show the results for $(Q^2 + E_\perp^2)/2$ and $2(Q^2 + E_\perp^2)^3$. Compared to the results of [18], the scale variations are somewhat tempered and are of the same order as that of the rather large experimental errors.

5 Conclusions

Using the latest structure and fragmentation functions, the complete NLO calculation of the direct and resolved contributions to forward particle production in deep inelastic scattering at HERA, describes the data rather well in the wide kinematical range available: $2\,\mathrm{GeV}^2 < Q^2 < 70\,\mathrm{GeV}^2$, $2.5\,\mathrm{GeV} < E_\perp < 15\,\mathrm{GeV}$. The importance of the NLO corrections to both the direct and resolved terms is pointed out. These large corrections are associated with new topologies involving gluon exchange in the hard subprocesses. These terms, which have no equivalent at the lowest order are interpreted as the first terms of the BFKL ladder. The data seem to indicate that resummation of such ladder diagrams is not necessary, probably because of the not so large rapidity phase space available. Agreement between theory and data is achieved choosing a standard scale of the form $(Q^2 + E_\perp^2)$. The variations under the proton factorization scale and the photon factorization scale are under control. However a rather large instability of the predictions is observed when varying independently the renormalization and the fragmentation scales. This prevents a really quantitative prediction for the single pion inclusive distribution in the forward region. In this respect, taking account of the HO resolved contribution improves the situation compared to calculations which ignored it but the situation is still far from satisfactory. We have checked that imposing a larger $E_\perp$ cut on the data reduces the scale sensitivity: for example, with the conditions $E_\perp > 7\,\mathrm{GeV}$ and $4.5\,\mathrm{GeV}^2 < Q^2 < 15\,\mathrm{GeV}^2$ the variation is $\pm^{13\%}_{10\%}$ for a scale variation as in Fig. 12. Probably, the evaluation of the next-to-next-to-leading order terms is required to obtain reliable and stable perturbative predictions.

---

[3] Note that the resolved photon scale differs slightly from the others since we use, as explained in Sect. 2, $M_\gamma^2 = (Q^2 + C_\gamma^2 E_\perp^2)$ with $C_\gamma^2 = 1/2$ and $C_\gamma^2 = 2$.

References

1. H1 Collaboration, A. Aktas et al., Eur. Phys. J. C **36**, 441 (2004) [hep-ex/0404009]
2. H1 Collaboration, C. Adloff et al., Phys. Lett. B **462**, 440 (1999) [hep-ex/9907030]
3. H1 Collaboration, (1996); (1997); (1997); C. Adloff et al., Nucl. Phys. B **538**, 3 (1999) [hep-ex/9809028]
4. ZEUS Collaboration, M. Derrick et al., Z. Phys. C **68**, 29 (1995) [hep-ex/9505011]
5. ZEUS Collaboration, J. Breitweg et al., Eur. Phys. J. C **11**, 251 (1999) [hep-ex/9903056]
6. H1 Collaboration, A. Aktas et al., Eur. Phys. J. C **37**, 141 (2004) [hep-ex/0401010]
7. ZEUS Collaboration, J. Breitweg et al., Eur. Phys. J. C **6**, 239 (1999) [hep-ex/9805016]
8. ZEUS Collaboration. J. Breitweg et al., Phys. Lett. B **479**, 37 (2000) [hep-ex/0002010]
9. A.L. Mueller, Nucl. Phys. (Proc. Suppl.) B **18**c, 125 (1990)
10. E.A. Kuraev, L.N. Lipatov, V.S. Fadin, Sov. Phys. JETP **45**, 199 (1977); I.I. Balitsky, L.N. Lipatov, Sov. J. Nucl. Phys. **28**, 822 (1978).
11. V.N. Gribov, L.N. Lipatov, Sov. J. Nucl. Phys. **15**, 438, 675 (1972); L.N. Lipatov, Sov. J. Nucl. Phys. **20**, 94 (1975);
    G. Altarelli, G. Parisi, Nucl. Phys. B **126**, 298 (1977);
    Y.L. Dokshitzer, Sov. Phys. JETP **46**, 641 (1977).
12. G. Ingelman, A. Edin, J. Rathsman, Comp. Phys. Comm. **101**, 108 (1997) [hep-ph/9605286]
13. H. Jung, Comp. Phys. Comm. **86**, 147 (1995).
14. J. Kwieciński, A.D. Martin, J.J. Outhwaite, Eur. Phys. J. C **9**, 611 (1999) [hep-ph/9903439]
15. A. Daleo, C.A. Garcia Canal, R. Sassot, Nucl. Phys. B **662**, 334 (2003) [hep-ph/0303199]
16. A. Daleo, D. de Florian, R. Sassot, hep-ph/0411212; A. Daleo, C.A. Garcia Canal, R. Sassot, Eur. Phys. J. C **33**, 404 (2004)
17. P. Aurenche, R. Basu, M. Fontannaz, R.M. Godbole, Eur. Phys. J. C **34**, 277 (2004) [hep-ph/0312359]
18. B.A. Kniehl, G. Kramer, M. Maniatis, hep-ph/0411300
19. M. Fontannaz, Eur. Phys. J. C **38**, 297 (2004) [hep-ph/0410021]
20. M. Drees, R.M. Godbole, J. Phys. G **21**, 1559 (1995) [hep-ph/9508221]
21. M. Glück, E. Reya, M. Stratmann, Phys. Rev. D **51**, 3220 (1995)
22. M. Glück, E. Reya, I. Schienbein, Phys. Rev. D **60**, 054019 (1999) [Erratum D **62**, 019902 (2000)] [hep-ph/9903337]
23. J. Chyla, M. Tasevsky, Phys. Rev. D **62**, 114025 (2000) [hep-ph/9912514]
24. A.D. Martin, R.G. Roberts, W.J. Stirling, R.S. Thorne, Eur. Phys. J. C **23**, 73 (2002) [hep-ph/0110215]
25. J. Pumplin, D.R. Stump, J. Huston, H.L. Lai, P. Nadolsky, W.K. Tung, JHEP **0207**, 012 (2002) [hep-ph/0201195]
26. B.A. Kniehl, G. Kramer, B. Pötter, Nucl. Phys. B **582**, 514 (2000) [hep-ph/0010289]
27. S. Kretzer, Phys. Rev. D **62**, 054001 (2000) [hep-ph/0003177]
28. G. Kramer, B. Pötter, Phys. Lett. B **453**, 295 (1999) [hep-ph/9901314]
29. H. Jung, L. Jonsson, H. Kuster, Eur. Phys. J. C **9**, 383 (1999) [hep-ph/9903306]
30. L. Bourhis, M. Fontannaz, J.P. Guillet, M. Werlen, Eur. Phys. J. C **19**, 89 (2001) [hep-ph/0009101]
31. M. Fontannaz, J.P. Guillet, G. Heinrich, Eur. Phys. J. C **26**, 209 (2002) [hep-ph/0206202]
32. L.H. Orr, W.J. Stirling, Phys. Rev. D **56**, 5875 (1997) [hep-ph/9706529]
33. J.R. Andersen, Acta Phys. Polon. B **33**, 3001 (2002) [hep-ph/0207019]